Locating the Anthropogenic Drivers of Urban Flooding from Centimetre-Resolution Aerial Imagery: A Reproducible Open-Data Pipeline for the Odaw Basin, Accra

Gideon Glago

Independent researcher

glagoegideon@gmail.com

This is a non-peer-reviewed preprint submitted to EarthArXiv. It has not been submitted to a journal for peer review. Subsequent versions may differ; readers should consult the repository below for the current state of the work and for the code and data underlying every figure and table reported here.

CORRESPONDENCE	Gideon Glago — glagoegideon@gmail.com

CODE AND DATA	https://github.com/osamabinIaggin/project-vision

CONFLICTS	None.
FUNDING	None.
VERSION	July 2026

Locating the Anthropogenic Drivers of Urban Flooding from Centimetre-Resolution Aerial Imagery: A Reproducible Open-Data Pipeline for the Odaw Basin, Accra

Gideon Glago · Independent researcher · glagoegideon@gmail.com

Project VISION · github.com/osamabinlaggin/project-vision · July 2026

ABSTRACT

Recurrent inundation in metropolitan Accra is, on the preponderance of the evidence, an anthropogenic rather than a climatological phenomenon: its proximate determinants are the obstruction of drainage by solid waste and the encroachment of structures onto watercourses. These determinants are metre-scale and therefore invisible to the moderate-resolution satellite imagery on which prior work has relied; municipal authorities presently enumerate them by pedestrian survey conducted after floods. This work develops a six-stage, fully reproducible pipeline that couples deep-learning semantic segmentation of centimetre-resolution aerial orthoimagery with terrain hydrology and open-channel hydraulics, using only openly licensed data, across five informal settlements of the Odaw catchment. Its scope is deliberately bounded: the system maps the built fabric and the drainage network, rates whether that network's measured geometry suffices, and tests the rating against independently documented flood history. Five results are reported. First, segmentation accuracy in this setting is bounded by label noise rather than model capacity; a cross-source *consensus verification* scheme — trusting only pixels on which two independent footprint sources agree, and excluding disputed pixels from loss and metric alike — establishes that the incumbent model was never deficient but mis-benchmarked, scoring 0.77 on verified pixels where it scored 0.58 against raw labels, and retraining under the corrected supervision reaches 0.80. Second, height above nearest drainage separates flood-reported localities from elevated controls at $p = 0.0074$ in a basin for which no flood extent has ever been published. Third, Manning conveyance analysis of 652 field-surveyed drain cross-sections finds the network is *not* undersized: 2.3% fails a conservative reference storm when clean, and siltation to three-quarters depth would multiply the failing length elevenfold to 25.8%. Fourth, that scenario is then measured rather than assumed — hand interpretation of 99 readable segments returns a mean surface obstruction of 0.29, so the elevenfold figure describes the network's *sensitivity* to siltation and not its present condition, under which one segment in ninety-nine fails. Fifth, cross-site degradation of the segmentation model is shown by leave-one-site-out testing to be a limitation of corpus coverage rather than a ceiling, recovering a mean of +0.287 IoU on unseen settlements. Five negative results are documented alongside, among them that reanalysis rainfall cannot supply a design storm for Accra, and that obstruction is not separable from overhead imagery at this resolution — a building-segmentation encoder discriminates blocked from clear channel at chance. Automated obstruction sensing is therefore scoped out of the present system and set out as future work, with the reasons quantified.

1. Introduction

The hydrological dysfunction of Accra is not principally a deficit of precipitation forecasting but a deficit of *spatial intelligence*. On 3 June 2015 a storm over the Odaw catchment killed approximately 150 people, most of them at a fuel station at Kwame Nkrumah Circle; the proximate cause identified in subsequent reporting was not the rainfall total but the failure of a drainage network choked with municipal refuse. That diagnosis has been repeated after every major event since, and the remedial instrument has remained constant: teams walk the drains after the water recedes and record what they find.

The central hypothesis of this work is that such enumeration can be performed *a priori*, automatically, and at scale, by interrogating sub-decimetre aerial imagery with a combination of semantic segmentation, terrain hydrology, and topology-aware geospatial reasoning. The hypothesis is attractive precisely because the causal mechanisms are small. A drain 0.5 m wide, half-filled with refuse, is a decisive hydraulic object and an entirely invisible one at the 30 m ground sampling distance of Landsat. It is legible at 5 cm.

Two constraints shaped the work throughout. The first is that no proprietary data were used: every input is openly licensed and every product is regenerated by a scripted acquisition step, because a method that depends on data the responsible agency cannot obtain is not a method it can adopt. The second is that negative results are reported as prominently as positive ones. Four substantive lines of enquiry failed during this project, and each failure constrains what a successor should attempt; they are given their own section rather than being omitted.

2. Study Area

The Odaw River drains a catchment of approximately 400 km² from the Akwapim foothills to the Korle Lagoon and thence to the Gulf of Guinea. Its lower reaches traverse the densest and most flood-exposed districts of metropolitan Accra. Five settlements within the catchment constitute the areas of interest.

Old Fadama / Agbogbloshie occupies the confluence of the terminal reach of the Odaw and the Korle Lagoon. As the hydraulic sink of the entire catchment it concentrates, within a tract of roughly 1.8 × 2.6 km, every mechanism under investigation: progressive colonisation of former wetland, dense riparian and on-drain construction, and chronic occlusion of the sea-outfall culverts. It was adopted as the pilot because it is the only site in Ghana with openly published drone orthomosaics at two epochs (2020 and 2024), permitting change detection.

Alogboshie, Akweteyman, Alajo and Nima lie upstream in the middle Odaw. They were added for two reasons. Their morphology differs materially from the lagoon-mouth fabric of Old Fadama, which makes them a genuine test of whether a model fitted at the outlet has learned anything transferable. And they are precisely the communities whose drains were surveyed segment-by-segment during the 2018–2020 Open Cities Africa and GARID field campaigns, making them the only places in the country where measured drain cross-sections and centimetre imagery coincide.

3. Data

All inputs are openly licensed. Raster payloads are excluded from version control and regenerated deterministically by the acquisition scripts.

Table 1. Data provenance. Every product is retrieved by a scripted acquisition step; none is redistributed in the repository.

Asset	Source	Licence	Specification
Orthomosaics (5 sites)	OpenAerialMap / Open Cities Africa	CC-BY 4.0	2.0–5.2 cm GSD, RGB
Building footprints	OpenStreetMap	ODbL	25,286 polygons (pilot AOI)
Building footprints	Google Open Buildings v3	CC-BY 4.0	~50 cm satellite-derived
Drain cross-sections	Open Cities / GARID field survey, via OSM	ODbL	2,107 ways; 760 with width and depth
Bare-earth terrain	FABDEM V1-2	CC-BY-NC-SA	30 m, buildings and forest removed
Built-up time series	Open Buildings 2.5D Temporal	CC-BY 4.0	presence, count, height; annual 2016–23
Radar	Sentinel-1 RTC (Planetary Computer)	open	20 m VV/VH gamma-nought
Rainfall	ERA5 hourly (Open-Meteo)	CC-BY 4.0	~31 km, 1980–2024

A structural observation about the terrain data governs much of what follows. No open product resolves Accra's ground micro-topography. FABDEM at 30 m is the open ceiling; the drone missions published orthomosaics but no surface models; Ghana has no national LiDAR, and the only airborne LiDAR known to exist over the basin is held internally by the GARID programme. Every methodological decision involving elevation in this work is a consequence of that ceiling rather than a preference.

4. Methods

The system is decomposed into loosely coupled stages rather than conceived as a monolithic end-to-end estimator. This is deliberate: the stages have different evidentiary standards, and a failure in one should be diagnosable without retraining the others. The decomposition also fixes the scope. Four stages establish the setting — the built fabric, the terrain hydrology, the encroachment overlay and its trajectory. The fifth rates whether the surveyed drainage geometry suffices. The sixth asks what the channels actually contain, and returns a measurement together with a bound on how far that measurement can be automated; it is reported as a scoping study for future work rather than as a delivered capability, for reasons quantified in §5.7.

4.1 Semantic segmentation and consensus-verified supervision

Orthomosaics are tessellated into 512 px tiles at 5 cm and resized to 256 px for a ResNet-34 encoder / U-Net decoder network[4,8], supervised by rasterised building footprints. The pilot corpus comprises 1,081 tiles over a 1,024 m window.

The central methodological problem emerged early: validation IoU plateaued near 0.58 while training loss continued to fall, and stronger recipes made it worse. Diagnosis established that the constraint was the supervision, not the network. OpenStreetMap footprints in dense informal fabric are offset by one to two metres and merge adjacent structures; Google Open Buildings[9] draws cleaner individual shapes but under-detects in the densest blocks. Rasterised onto an identical grid, the two sources agree at only IoU 0.611 — the empirical noise floor of the labels.

The resolution adopted here is *consensus verification*. Where the two independent sources agree, whether on building or on background, the label is trusted. Where they disagree — 23% of pixels — the pixel is marked *ignore* and excluded from the loss and from the metric alike. This is not label fusion: no attempt is made to adjudicate the disputed pixels. It is an admission that the project does not know their true value, encoded so that neither training nor evaluation pretends otherwise.

4.2 Terrain hydrology

Height above nearest drainage (HAND)[7] is derived over the full catchment with WhiteboxTools[6]: least-cost depression breaching, D8 flow accumulation, stream extraction at a 2.7 km² support threshold, then normalisation of elevation to the nearest stream cell. FABDEM is used rather than raw Copernicus GLO-30 because over dense urban fabric the raw surface embeds roof heights and corrupts flow routing[3].

4.3 Encroachment overlay and temporal trend

Encroachment is adjudicated deterministically, without a learned model, as the intersection of building footprints with buffers about mapped drain centrelines and water polygons. Because any such tally is a monotone function of the chosen tolerance, a sensitivity sweep is reported rather than a single figure. Multi-temporal built-up trend is taken from Open Buildings 2.5D Temporal, which supplies eight consistent annual epochs from a single model — replacing a two-epoch drone difference that proved dominated by inter-flight prediction flicker.

4.4 Conveyance hydraulics

For each surveyed drain segment, full-section conveyance is computed by the Manning equation[1], $Q = (1/n)\, A\, R^{2/3}\, S^{1/2}$, with cross-sectional area and hydraulic radius derived from the surveyed profile (rectangular, trapezoidal, elliptical, or rectangular-with-rounded-invert), and roughness from surveyed material and invert smoothness.

Two departures from textbook practice were forced by the data and are material to the result. First, no design storm is used. Section 6 documents why reanalysis rainfall cannot supply one for Accra; instead the rational method is inverted to solve for each segment's *critical intensity*, $i_{\text{crit}} = Q_{\text{cap}} \cdot 3.6{\times}10^6 \,/\, (C A)$, the rainfall rate at which that drain reaches capacity. This is a property of the drain and its catchment alone, requiring no rainfall input and no return period, and it renders the resulting ranking invariant to the missing intensity–duration–frequency relation. Second, contributing area is accumulated on the drain network itself rather than routed over the DEM, because a 30 m surface cannot determine which side of a street drains to which gutter. Each 10 m cell is allocated to its nearest drain by chamfer propagation, and local catchments are accumulated downstream through the network graph, reconstructed from OSM endpoints snapped at 3 m and oriented by a 300 m-smoothed elevation field.

Longitudinal grade is measured across a 300 m chord and clamped to the range urban drains are laid to (0.1–2%); the DEM places a segment within that range but is never permitted to assert a grade outside it. Since grade enters as $S^{1/2}$, the ranking is invariant to the choice and only absolute counts shift.

4.5 Corridor sampling and channel interpretation

Because the surveyed geometry is known, the channel need not be searched for: each centreline is walked at 20 m and a 10 × 6 m chip cut about the station, rotated by the local bearing so the channel runs consistently across the frame. This is a materially easier sampling problem than blind tiling, and it is what makes hand interpretation of a randomly drawn subset affordable. Each chip is scored for whether the channel is visible at all and, if so, for surface obstruction on a four-point scale; a blind re-read of a held-back portion establishes the reliability ceiling against which any automated method must be judged. Scene assignment uses each mission's traced flown footprint rather than its catalogue bounding box, the two differing by enough at one site to misroute 150 segments to imagery that does not cover them.

4.6 Cross-site evaluation protocol

Generalisation is measured by leave-one-site-out: a site is withheld *entirely*, the model is fine-tuned on the remaining four, and the withheld site is scored under the identical verified-pixel metric. Withholding whole sites rather than random tiles is what makes this a test of transfer rather than of interpolation — tiles drawn from a single 512 m window are far too spatially correlated for a random split to say anything about a new settlement.

5. Results

5.1 Segmentation is label-bound, not capacity-bound

On an identical 1,081-tile split, a pretrained ResNet-34 encoder outperformed a from-scratch U-Net, 0.579 against 0.530 validation IoU. Attempts to improve on that by optimisation were uniformly unsuccessful: native-resolution multi-scale crops, photometric jitter, differential encoder/decoder learning rates and an AdamW warmup-cosine schedule over a 60-epoch budget scored *below* the baseline, at 0.561 and 0.566. The added capacity was memorising label noise. A global-shift registration search over the OSM mask peaked at 0.2 m, establishing that the label error is per-building and random rather than a correctable systematic offset. The one genuine post-hoc gain was inference-time: four-way flip test-time augmentation with a calibrated threshold lifted the baseline to 0.593 at zero training cost.

Consensus verification changed the picture qualitatively rather than incrementally.

> **Scored on verified pixels only, the existing transfer-learning model achieves pooled IoU 0.77.** Most of its apparent error had been disagreement with label noise, not with reality. Retraining with disputed pixels masked out of the loss yields a further genuine gain to **0.80 pooled** (0.70 per-tile), and the resulting model correctly rejects OSM's phantom buildings on open ground — for which its legacy score against raw OSM masks *falls* to 0.55.

That last detail is worth dwelling on, because it is the strongest evidence that the metric rather than the model had been at fault. A model that improves on reality while scoring worse against the labels is a model whose labels are wrong. Reporting the legacy figure alone would have registered the improvement as a regression.

Figure 1. Predictions from the consensus-trained model on held-out tiles. The model produces coherent region-level built-up extent; per-footprint delineation in the dense core remains bounded by label granularity and would require instance-level annotation to address.

Figure 2. The two independent label sources over identical ground. Left, OpenStreetMap (red); right, Google Open Buildings v3 (cyan). OSM is dense but offset and merges adjacent structures; Open Buildings draws cleaner shapes but under-detects in the densest blocks. Their mutual agreement of IoU 0.611 is the empirical noise floor against which any model score must be read.

5.2 Cross-site degradation is a coverage limitation, not a ceiling

Applied zero-shot to the four upstream communities, the pilot checkpoint degrades substantially: pooled verified IoU falls from 0.798 to 0.523. The interpretation of that fall depends entirely on a quantity that is easy to omit — the label-noise floor at the new sites, which moves only from 0.611 to 0.578. Because the score moves an order of magnitude further than the floor, the loss is attributable to the model rather than to worse supervision upstream. A control run scoring the pilot's own validation split through the identical code path recovered 0.798 against the 0.80 published from the original training, confirming that the transfer number measures transfer and not a pipeline defect.

One site, Alogboshie, degraded far beyond the others, to 0.298, under-segmenting by more than three-fold. A preprocessing explanation was the obvious suspect and was tested rather than assumed: it is the finest source at 2.01 cm and must be reduced 2.49× to reach the training resolution, where the other three are reduced by 1.55×, 1.39× and 1.04×, and bilinear resampling under-filters beyond a factor of two. Re-fetching with area-average resampling moved the score from 0.297 to 0.298. The hypothesis is refuted; the difficulty is a real domain difference.

Leave-one-site-out then established that the gap is learnable.

Table 2. Leave-one-site-out generalisation. Each site is withheld entirely and the model fine-tuned for eight epochs on the remaining four. Held-in performance is reported to exclude catastrophic forgetting as an explanation for any gain.

Held-out site	Tiles	Before	After	Change	Held-in
Alogboshie	377	0.298	**0.616**	+0.318	0.885
Nima	400	0.507	**0.863**	+0.355	0.866
Alajo	398	0.603	**0.833**	+0.231	0.888
Akweteyman	400	0.641	**0.883**	+0.242	0.881
Old Fadama †	1,081	0.904	0.681	—	0.912

† Not comparable. The starting checkpoint was fitted on 80% of these tiles, so the "before" figure is a training-set score and the apparent decline is contamination rather than regression. The interpretable quantity in that fold is the 0.681 which four upstream communities alone generalise to Old Fadama, having never seen it.

Every genuinely unseen site improves, by between 0.231 and 0.355 for a mean of **+0.287**, without the model ever seeing a tile from the site on which it is scored. Held-in performance remains between 0.866 and 0.912 throughout, so none of the gain is bought by forgetting. A production checkpoint fitted on all 2,656 verified tiles scores 0.880 pooled on its validation split, distributed evenly across sites (0.862 to 0.912); that figure measures fit rather than generalisation and the leave-one-site-out result remains the honest expectation for a settlement outside the corpus.

Alogboshie is the informative case, and its trajectory states the argument in a single site: **0.298 unseen, 0.616 held out with four siblings present, 0.868 represented in training.** Its difficulty was never intractable — only unrepresented.

Figure 3. Zero-shot transfer to the four upstream communities, one row per site: imagery, verified label (blue; grey denotes ignore pixels), and prediction. Under-segmentation at Alogboshie is visible as sparse predicted extent against dense actual fabric.

5.3 Hydrological hazard

No agency has published a flood extent for any Odaw event: UNOSAT's only Ghana product covers the October 2023 lower-Volta event, verified here to lie outside the basin; the 2015 event is absent from the Global Flood Database; Copernicus EMS was never activated. Validation therefore proceeds on primary data.

Every Odaw-basin locality named in multi-year flood reporting — Old Fadama, Circle, Odawna, Adabraka, Kaneshie, Nima, Alajo, Abeka Lapaz — was compared against eight elevated control districts absent from that reporting, geocoded independently via OSM Nominatim. Median HAND is **1.9 m against 23.0 m**, AUC 0.86, exact one-sided Mann–Whitney $\boldsymbol{p}$ **= 0.0074**. The two flooded localities that sampled high are centroid artefacts — Nima and Lapaz geocode to ridge tops above their valley frontage — and were retained precisely because they bias against the hypothesis.

The integrated exposure product yields a flat and uncomfortable statement: the entire 37.7 ha of model-delineated built-up Old Fadama lies below 2 m HAND, at a mean of 0.03 m. Within-AOI hazard gradation is physically absent rather than merely unresolved, and no finer classification should be manufactured to suggest otherwise.

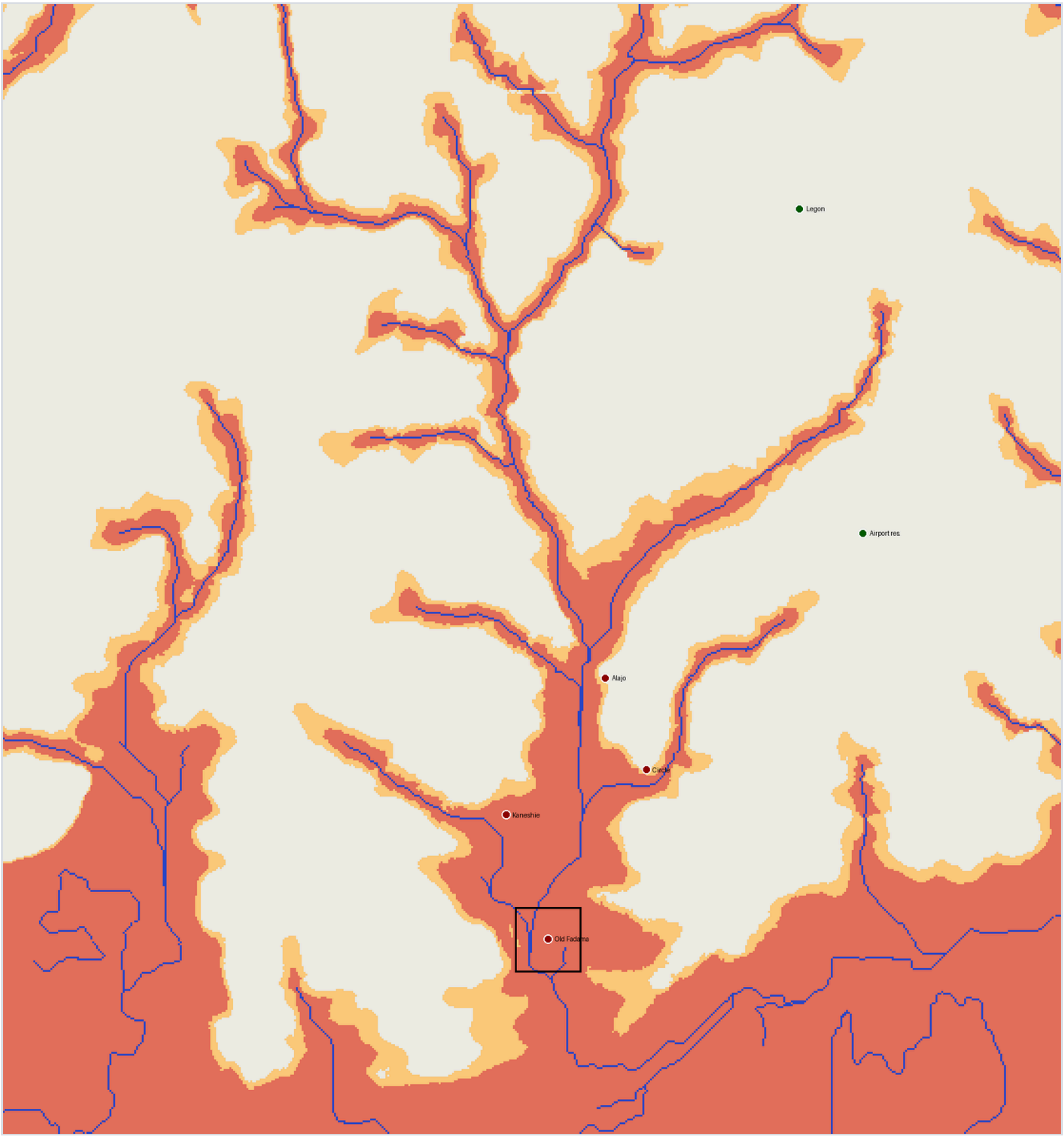

Figure 4. HAND hazard classes over the lower Odaw corridor. Red denotes severe (<2 m), amber moderate (2–5 m), pale marginal (≥5 m); the drainage network is shown in blue, documented 2015 flood sites as dark circles and elevated controls as green. The pilot AOI is outlined; it lies wholly within the severe class.

5.4 Encroachment and its trajectory

The deterministic overlay adjudicates two modalities of encroachment within the 2020 epoch: on-drain construction and riparian construction. At a 5 m tolerance 114 structures intersect a mapped drain or canal; the union of drain-5 m and water-10 m criteria gives **273 structures**. No structure lies within a mapped water polygon, an internal consistency check on the geometry.

The multi-temporal series supplies the trajectory. Built-up area within the AOI grew from 22.4 to 33.3 ha between 2016 and 2021, contracted to 27.4 ha in 2022, and rebounded to 30.0 ha by 2023; built-up area within a 15 m riparian buffer grew **tenfold**, from 0.03 to 0.31 ha. The contraction is itself a validation of the source: the epochs are dated 30 June, and the police-backed Agbogbloshie clearance began 1 July 2021, so the series falls in exactly the epoch it must and recovers as documented reoccupation proceeded. Mean structure height holds at 5–6 m throughout, confirming minimal vertical refuge.

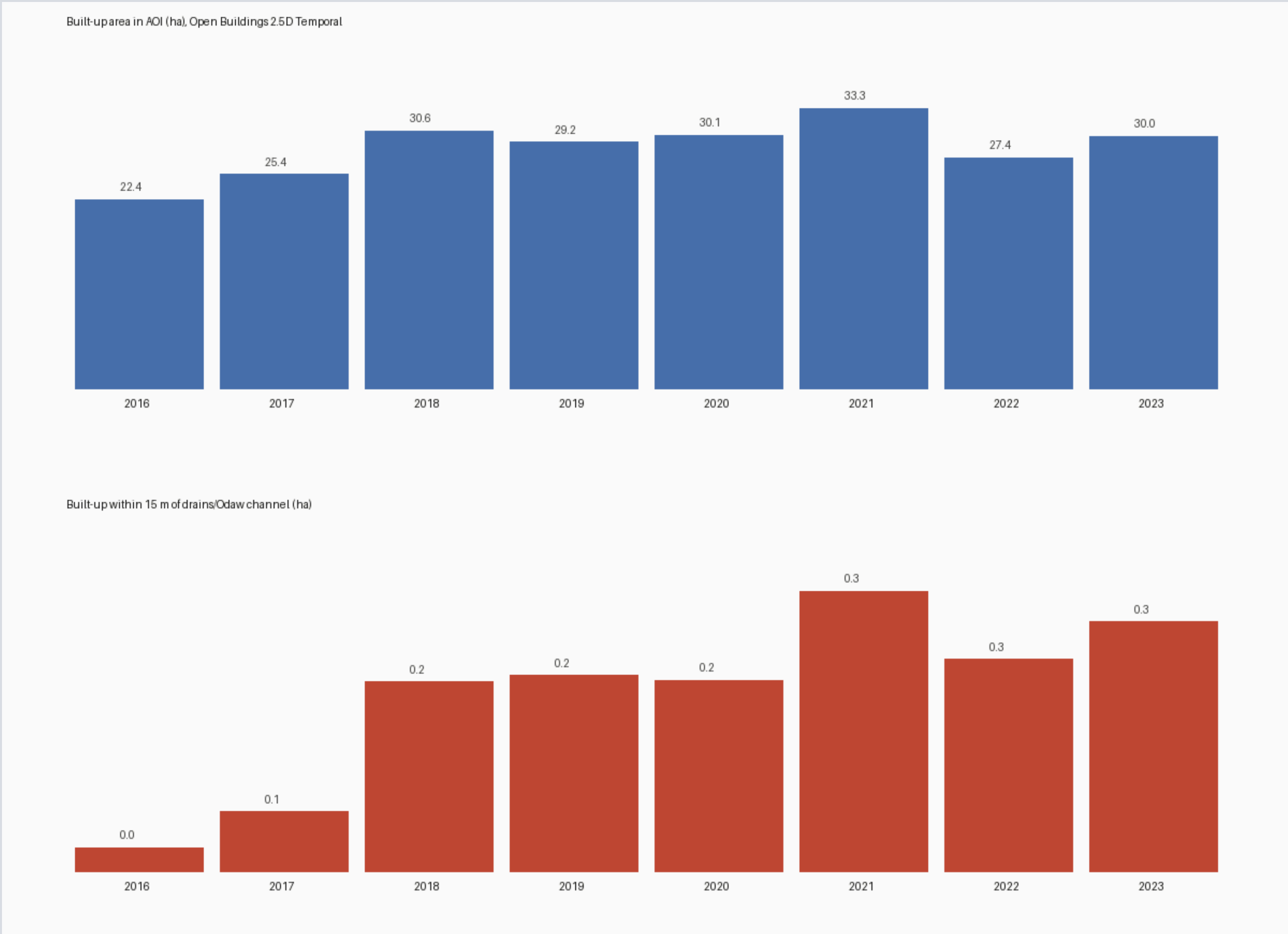

Figure 5. Annual built-up area (upper) and built-up area within 15 m of the drainage network (lower), 2016–2023. The 2021→2022 contraction coincides with the documented July 2021 clearance; riparian encroachment grows an order of magnitude across the series.

5.5 The drains are not undersized

Two data findings preceded any hydraulic result and materially changed it. First, 108 surveyed segments carry widths of 4–20 cm — median 6 cm — against depths of 0.2–0.7 m, aspect ratios reaching 13:1. These are not street drains but unit or entry errors in the field campaign, and left in they supplied 91 of the 107 apparently critical segments and dominated the ranking entirely. They are flagged in the published output and held out of the headline statistics rather than silently discarded. Second, the surveyed network is topologically fragmented — 484 connected components before endpoint snapping, 293 of them isolated single ways — so accumulated catchments remain local, at a median of 0.64 ha, and no trunk conveyance is represented.

On the 652 segments (45.2 km) with credible geometry, the result inverts the expected finding.

Table 3. Network failing a 20.8 mm/h reference storm as a function of invert condition. The reference is the ERA5 one-hour ten-year intensity, a figure known to understate Accra's true intensities, so every share reported is a lower bound.

Invert condition	Segments failing	Length	Share of network
Clean section	16	1.0 km	2.3%
25% silted	27	1.9 km	4.1%
50% silted	46	3.1 km	6.9%
75% silted	146	11.6 km	**25.8%**

> At full section the median segment conveys 0.61 m^3/s against a median catchment of 0.64 ha and tolerates 309 mm/h — an intensity no Accra storm approaches. **Capacity is lost to the state of the invert, not to its geometry.** Siltation to three-quarters depth multiplies the failing length elevenfold; the median segment fails once 85% silted, and the most fragile fifth at 36%.

The policy reading is direct and runs against intuition. The instinctive response to a flooded city is to build larger drains; on this evidence the drains that exist are adequate for their local catchments when clean, and the binding constraint is the state of the invert. That relocates the intervention from capital works to maintenance.

Two cautions attach to the table, and the second is the subject of §5.6. The siltation column is a *scenario*: it states what would happen at a given blockage, not what blockage obtains. And the elevenfold figure is a statement about the network's **sensitivity** to siltation, which is not the same claim as a description of its present condition. Read as the latter it would assert that a quarter of the surveyed network is currently failing, which the following section shows it is not.

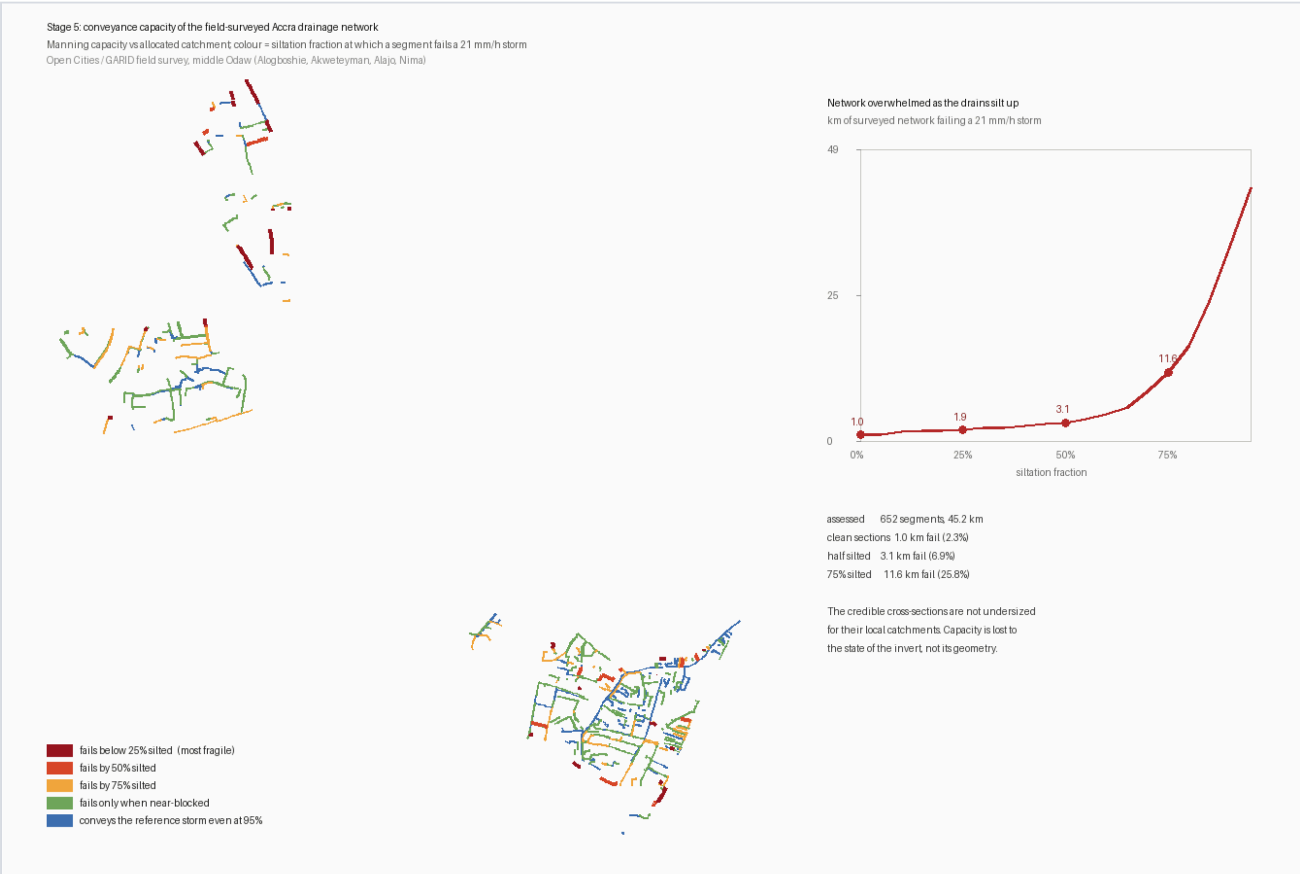

Figure 6. Left, the surveyed network coloured by the siltation fraction at which each segment fails the reference storm; red segments are the most fragile. Right, network length failing as a function of siltation, showing the sharp non-linearity beyond half-blockage.

5.6 The siltation scenario, measured — and why it cannot be automated

A capacity model whose decisive parameter is a swept scenario invites the question of what that parameter actually is. Corridor imagery was therefore cut along the surveyed centrelines and read by hand. One hundred and fifty segments were sampled at random (9.0 km, 19.9% of the assessed network); on 99 of them (6.0 km) the channel could be seen at all. Across those, surface obstruction is **median 0.25, mean 0.29, 95% CI 0.23–0.34** — between the 25% and 50% levels of the Stage-5 sweep and nowhere near 75%. Re-rating the readable segments at what was observed rather than at a scenario, **one of ninety-nine fails the reference storm, against twenty-three under the 75% case**.

This is the substantive correction to §5.5, and it cuts both ways. The network is in better condition than the alarming end of the sweep implies; but its fragility is unaltered, because fragility is a property of the geometry and the geometry has not changed. The honest statement is that the drains are presently coping and would stop coping under a degree of siltation that is neither implausible nor currently observed.

The obstruction figure is a **lower bound** for a reason intrinsic to the sensor. Overhead imagery sees the channel surface. Refuse bridging an otherwise clear void overstates the blockage; silt lying beneath standing water is invisible and understates it — and silt is precisely what the Manning roughness term responds to.

5.7 Obstruction is not separable at this resolution

Automating the interpretation was then attempted and failed, and the failure is reported in the same detail as a success would have been. Segments were held out whole. Reliability was measured first, by blind re-reading of 90 chips: 0.851 agreement (κ = 0.698) on clear-versus-obstructed, 0.922 on visible-versus-not. Being an intra-annotator test–retest by a single interpreter, that is an upper bound on what any model could be scored against.

Table 4. Discrimination on held-out segments, against a reliability ceiling of 0.851. The two tasks separate cleanly: whether the channel can be *seen* is learnable; whether it is *blocked* is not.

Model	Channel visible (AUC)	Channel obstructed (AUC)
Majority baseline	0.500	0.500
Photometric (16 hand-built features)	**0.701**	0.626
Stage-2 production encoder, frozen	0.677	**0.510**

The encoder result is the sharper one. In §5.2 a building representation transferred *imperfectly* to unseen settlements; here, on imagery of the same ground, it carries **no signal at all** about what lies inside a channel — 0.510 against a 0.500 baseline. A model trained to find roofs has learned nothing that distinguishes refuse from water from concrete. Three candidate rescues were eliminated rather than assumed: finer imagery does not help (photometric discrimination improves at ≤3.6 cm while the encoder's *degrades*, and the effect does not survive a change of feature set); the learning curve is flat from 39 to 99 labelled segments, so the constraint is not sample size; and the most severe class is too rare to learn — 6 chips in 300 — because the mass of obstruction sits in an ambiguous middle rather than at the extremes.

Consequently the model's estimate is published in its own column and is **never merged into the hand readings**. A near-chance classifier propagated through a hydraulic model would acquire, from the precision of the arithmetic downstream of it, an authority it has not earned.

There is a reason to think per-station classification is the wrong target, independent of resolution. A reach floods at its *controlling section*: one blocked culvert mouth backs water up through a hundred metres of otherwise clear channel. A segment mean — the statistic computed here — is therefore not the quantity that governs, and even a perfect station-level classifier would be answering a subtly different question from the one that matters. This also supplies a benign reading of the interpreter's own 0.851 ceiling: judging a 10 m window in isolation is genuinely ill-posed when the hydraulically decisive feature may lie just outside it.

Observability, not accuracy, is the operative ceiling. Only 60% of stations on drains the survey itself records as *open* could be read, the remainder lost to roof overhang, building lean in the orthomosaic, tree canopy and deep shadow. That is well below the ~82% implied by the culvert tagging alone, and it bounds any overhead method regardless of model quality. One flaw in the present protocol is recorded rather than absorbed: the annotation contact sheets displayed the surveyed `covered` tag, so the covered-versus-open observability contrast is partly circular; the sole genuinely blind cross-check available, `material_smoothness`, is null (t = 0.77). The obstruction reading therefore rests on the hand labels and their test–retest, and on nothing further.

6. Negative results

Five lines of enquiry failed. Each is reported because it constrains what a successor should attempt.

Reanalysis rainfall cannot supply a design storm for Accra. A Gumbel relation fitted to 45 years of ERA5 hourly precipitation[5] is internally well-behaved and reproduces the city's annual total of roughly 900 mm. It is nonetheless unusable: on every documented flood day the reanalysis returns a depth *below every annual maximum in the record*, rendering the lethal 3 June 2015 storm as a 5.1 mm/h, 10.8 mm/24 h day. Six sample points spanning the metropolis return byte-identical series, confirming that this is grid resolution and not storm displacement — one ~31 km cell covers the city, and coastal Accra's convective rainfall lies beneath it. This finding forced the inversion of the hydraulic model described in §4.4, and is the reason no absolute return-period statement appears in this work.

Open-water SAR is physically blind in this floodplain. Sentinel-1 RTC scenes were processed for the 18 June 2018 and 9 June 2020 events against dry-season reference stacks. The detector is demonstrably sound — it maps 121 ha of water change on 9 June 2020 at 99.5% below 2 m HAND, AUC 0.95 — but that signal is dominated by the Panbros salt-pan cycle, which serves as a positive control. Inside the Odaw floodplain it detects almost nothing: the surface is near-continuously roofed, and flooded streets *raise* VV backscatter through double-bounce rather than darkening it.

The complementary urban double-bounce channel is equally null. Across all 29 June acquisitions from 2015 to 2024, the single same-evening flood acquisition ranks fifth on floodplain backscatter anomaly (p = 0.17), and the anomaly does not correlate with pre-pass rainfall (Spearman $\rho = -0.02$). At 20 m VV gamma-nought there is no usable flood signal here by either mechanism.

Stronger training recipes degrade accuracy under label noise. Documented in §5.1: aggressive augmentation and extended optimisation schedules scored below a plain baseline, because the additional capacity was spent memorising label error. On label-noisy corpora the productive intervention is on the supervision, not the recipe.

Overhead imagery cannot classify drain obstruction at this resolution. Documented in §5.7: a photometric model reaches AUC 0.626 and the project's own production segmentation encoder reaches 0.510 — chance — against an interpreter ceiling of 0.851, with finer imagery, more labels and class rarity each eliminated as the explanation. The negative is doubly informative, because the same models discriminate whether the channel is *visible* at AUC 0.70: the imagery supports one judgement about the corridor and not the other. Sensing that would plausibly help is oblique or street-level acquisition that sees into the channel rather than onto it, multi-temporal differencing of the same corridor, which converts an absolute judgement into an easier relative one, or acquisition immediately after rainfall, where standing water in a drain that ought to be flowing is a stronger and more directly hydraulic signal than refuse texture.

A sixth hypothesis, that Alogboshie's transfer failure was a resampling artefact, was tested and refuted in §5.2. It is recorded here because the temptation to accept it was considerable: the resampling factors ranked the four sites in exactly their score order, which is precisely the kind of coincidence that survives casual scrutiny.

7. Discussion

The two findings with the widest applicability are methodological rather than geographic.

The first is consensus verification. Its premise is that when two independent label sources disagree, the honest response is neither to pick one nor to average them but to decline to score the disagreement. The gain here was substantial — from an apparent 0.58 to a measured 0.80 — but the more consequential effect was diagnostic: it revealed that a model believed to be mediocre had been performing well against a benchmark that was wrong. The conditions for applying it are common. OpenStreetMap and Open Buildings jointly cover most of the Global South, they fail in different and largely uncorrelated ways, and any project training a segmentation model on either alone is measuring its model against those failures.

The second is the discipline of reporting a label-noise floor beside every score. A drop in IoU on a new site is uninterpretable in isolation: it may indicate a model that failed to transfer, or supervision that is simply worse there. This project made the corresponding error once in the opposite direction, briefly reading a legacy score of 0.55 as a regression when it was evidence of improvement, and the protocol adopted thereafter — report the floor with the score, always — is what made the cross-site result legible.

The domain finding of §5.5 carries the clearest operational implication. If the surveyed drains are adequate when clean, then the quantity that determines whether a neighbourhood floods is one that changes on the timescale of a wet season, is invisible to any cross-section survey, and is in principle observable from overhead imagery. That is a considerably more tractable target than the capital programme the intuitive diagnosis implies, and it is the point at which the two halves of this work — the segmentation and the hydraulics — converge on a single measurement.

8. Limitations

- **The obstruction measurement is thin and partly unblinded.** It rests on 99 readable segments read by a single interpreter, with a test–retest in place of a second annotator, and the one genuinely blind cross-check available is null. It is a lower bound besides: overhead sensing cannot see silt beneath standing water, which is the material the roughness term responds to.
- **Observability, not model accuracy, bounds any overhead method.** Only 60% of stations on drains the survey records as open could be read; with covered and culverted reaches counted the practical ceiling falls well below the ~82% the tagging alone implies.
- **A segment mean is not the governing quantity.** A reach floods at its controlling section, so averaging obstruction along a segment understates the effect of one severe local blockage. Addressing this requires obstruction located along the reach rather than summarised over it, which the present sampling does not provide.
- **Trunk conveyance is absent.** The surveyed network is fragmented and represents tertiary street collectors; basin-scale backwater, a documented contributor at the Odaw outfall, lies outside the model.

- **Every intensity is anchored to a floor known to understate the truth** (§6), so absolute failure shares are lower bounds and no return-period claim is made.
- **Longitudinal grades are constrained, not measured** — bounded to engineering practice rather than surveyed — though the ranking is invariant to the choice.
- **Per-footprint delineation remains bounded by label granularity.** Additional sites do not address it; instance-level annotation would be required.
- **Alogboshie remains the hardest site even when represented in training**, so settlement morphology continues to cost accuracy and a single model across heterogeneous fabric is not free.

9. Reproducibility

The pipeline is implemented as thirty-three numbered scripts executed in sequence, each performing one acquisition or analysis step and each documenting its own rationale, including the steps that failed. One class of product is necessarily irreproducible and is therefore versioned rather than regenerated: the hand channel interpretations of §5.6, which no rerun can recreate. Large rasters are excluded from version control and regenerated by the acquisition scripts; the repository versions the methodology rather than the payload. Remote cloud-optimised imagery is read by windowed range request rather than bulk download, so reconstructing the five-site corpus transfers roughly 1% of the 2.5 GB the scenes nominally occupy. All analysis outputs are published as CSV and GeoPackage alongside the figures reproduced here.

10. Conclusion

Centimetre-resolution aerial imagery, combined exclusively with openly licensed ancillary data, supports a specific and bounded claim about the Odaw basin. It delineates the built fabric at 0.80 verified IoU and generalises that delineation to settlements it has not seen; it ranks hydrological hazard against a terrain criterion that separates flood-reported from control localities at $p = 0.0074$; it enumerates encroachment on the drainage network and measures its decadal growth; and it rates the measured geometry of that network, finding it adequate for its local catchments when clean, presently obstructed to a mean of 0.29, and steeply sensitive to further siltation. Mapping the drainage and adjudicating its sufficiency is therefore within reach of open data. Sensing the *contents* of the channel is not.

That boundary is drawn from measurement rather than from caution. Obstruction proved unseparable from overhead imagery at this resolution — a building encoder discriminates blocked from clear channel at chance — and only three-fifths of nominally open drains can be read at all. Both findings are quantified in §5.7 rather than deferred, because they define where the next increment of effort should go: not to more labels or finer orthomosaics, each of which was tested and neither of which helped, but to sensing that sees into the channel rather than onto it, and to locating obstruction along a reach rather than averaging it over one, since a reach floods at its controlling section.

Two constraints on that future work are worth stating plainly, since both bear on how the present result should be extended. There is no water-level record for these drains, nor for any drain in the catchment; the validation anchor available is documented flood *occurrence* at locality level, which is what §5.3 uses and what a hydraulic rating can presently be tested against. And a probabilistic statement — how a given blockage shifts the likelihood of flooding at a given place — requires both that record and an obstruction observation the imagery cannot yet supply. The contribution of this work to that programme is to have established which of its components are already tractable, and to have measured, rather than assumed, the difficulty of the one that is not.

References

1. Chow, V. T. (1959). *Open-Channel Hydraulics*. McGraw-Hill, New York.
2. Chow, V. T., Maidment, D. R., & Mays, L. W. (1988). *Applied Hydrology*. McGraw-Hill, New York.
3. Hawker, L., Uhe, P., Paulo, L., Sosa, J., Savage, J., Sampson, C., & Neal, J. (2022). A 30 m global map of elevation with forests and buildings removed. *Environmental Research Letters*, 17(2), 024016.
4. He, K., Zhang, X., Ren, S., & Sun, J. (2016). Deep residual learning for image recognition. *Proceedings of the IEEE Conference on Computer Vision and Pattern Recognition*, 770–778.
5. Hersbach, H., et al. (2020). The ERA5 global reanalysis. *Quarterly Journal of the Royal Meteorological Society*, 146(730), 1999–2049.
6. Lindsay, J. B. (2016). Whitebox GAT: A case study in geomorphometric analysis. *Computers & Geosciences*, 95, 75–84.
7. Nobre, A. D., Cuartas, L. A., Hodnett, M., Rennó, C. D., Rodrigues, G., Silveira, A., Waterloo, M., & Saleska, S. (2011). Height Above the Nearest Drainage — a hydrologically relevant new terrain model. *Journal of Hydrology*, 404(1–2), 13–29.
8. Ronneberger, O., Fischer, P., & Brox, T. (2015). U-Net: Convolutional networks for biomedical image segmentation. *MICCAI 2015*, LNCS 9351, 234–241.
9. Sirko, W., et al. (2021). Continental-scale building detection from high-resolution satellite imagery. *arXiv:2107.12283*.

 Imagery courtesy of OpenAerialMap contributors and the Open Cities Africa programme; drain survey attributes courtesy of the Open Cities Accra / GARID field campaigns via OpenStreetMap contributors.